Few-shot Learning-based, Long-Term Stable, Sensitive Chemosensor for On-Site Colorimetric Detection of Cr(VI)

Zhao-Jing Huang [†, ⁄⁄], Hao Li [‡, ⁄⁄], Jia-Yi Luo [†],Shunxing Li [†,§,*], Fengjiao Liu [†,§,*]

[†] *College of Chemistry, Chemical Engineering & Environmental Science, Minnan Normal University, Zhangzhou 363000, China.*

[‡] *School of Electrical and Data Engineering, Faculty of Engineering and IT, University of Technology Sydney, Sydney, 2007, Australia*

[§] *Fujian Province Key Laboratory of Modern Analytical Science and Separation Technology, Fujian Province University Key Laboratory of Pollution Monitoring and Control, Minnan Normal University, Zhangzhou 3630003, China*

***Corresponding Author**

Prof. Dr. Li Shun-xing

E-mail: lishunxing@mnnu.edu.cn

Fax : +86-596-2591395

ABSTRACT: The rapid emergence of deep learning, e.g., deep convolutional neural networks (DCNNs) as one-click image analysis with super-resolution, has already revolutionized colorimetric determination. But it is severely limited by its data-hungry nature, which is overcome by combining the generative adversarial network (GAN), i.e., few-shot learning (FSL). Using the same amount of real sample data, i.e., 414 and 447 samples as training and test sets, respectively, the accuracy could be increased from 51.26 to 85.00%, because 13,500 antagonistic samples are created and used by GAN as the training set. Meanwhile, the generated image quality with GAN is better than that with the commonly used convolution self-encoder method. The simple and rapid on-site determination of Cr(VI) with 1,5-diphenylcarbazide (DPC)-based test paper is a favorite for environment monitoring but is limited by unstable DPC, poor sensitivity, and narrow linear range. The chromogenic agent of DPC is protected by the blending of polyacrylonitrile (PAN) and then loaded onto thin chromatographic silica gel (SG) as a Cr(VI) colorimetric sensor (DPC/PAN/SG); its stability could be prolonged from 18 h to more than 30 days, and its repeatable reproducibility is realized via facile electrospinning. By replacing the traditional Ed method with DCNN, the detection limit is greatly improved from 1.571 mg/L to 50.00 μg/L, and the detection range is prolonged from 1.571-8.000 to 0.0500-20.00 mg/L. The complete test time is shortened to 3 min. Even without time-consuming and easily stained enrichment processing, its detection limit of Cr(VI) in the drinking water can meet on-site detection requirements by USEPA, WHO, and China.

KEYWORDS: *chromium, intelligent detection, colorimetric analysis, deep learning*

Introduction

In recent years, many exciting discoveries have been reported through the cross-application of various disciplines and deep learning (DL).[1-2] Analytical chemistry, in particular, has successfully benefited from the application of DL tools for extracting qualitative and quantitative information from high-dimensional and complex chemical measurements.[3] The deep convolutional neural network (DCNN), artificial neural network, support vector machine, and generative adversarial network (GAN) are some examples of DL algorithms frequently employed in chemical analysis. Currently, DCNN has been successfully applied to improve the analytical performance of APP-based colorimetric determination, including denoising, recognition, and summary of every small characteristic change from each image.[4,5] However, data-driven DCNN is data-hungry. A large number of samples are typically required for proper learning, which has been the major challenge of its application in analytical chemistry for its time-consuming and resource-greedy part, i.e., “time and money” cost.[3,6] Often, this is a serious problem. If a training data set is inadequate for the desired task, the resulting model generalization will be insufficient, and then the accuracy will be low.[7] Typically, the solution to data hunger is through operations such as cutting and rotating sample images, but this is inapplicable to the data from chemical analysis. Therefore, we propose a scheme based on GAN. As a new semisupervised learning and unsupervised learning technology, GAN can generate a large number of real sample-based antagonistic samples, i.e., "fake samples", with the same pattern by learning a small number of real samples and implicitly modeling the distribution of potential samples.[8,9] The essence of its training process is a pair of network competition processes to get back propagation signals to achieve the goal. Using this few-shot learning model (FSL), tens of thousands of antagonistic sample can be simulated through the study of hundreds of real samples with obvious characteristics, and then the challenge of data-hungry

DCNN could be overcome.

Another challenge to data quality from chemistry aspects is mainly from the stability of the sensor. To assess the performance of the FSL model in chemical analysis, it is necessary to construct a stable chemical sensor to obtain high-quality sample data. With the increasing concern for human health and hydrosphere protection, the toxicity of Cr(VI) as a powerful carcinogenic agent has been widely recognized, and then Cr(VI) is listed as a priority pollutant by many countries, including the USA and China.[10,11] Because Cr(III) can be transformed into toxic Cr(VI) by the pathway of photooxidation in natural environments, chromium emission and its content in drinking water and industrial wastewater should be strictly restricted.[12] Therefore, the maximum acceptable concentration for soluble chromium in drinking water is set at 100 μg/L by the United States Environmental Protection Agency (USEPA), and a more strict threshold (50 μg/L) is set by the World Health Organization (WHO) and China.

The conventional analysis of Cr(VI) in water requires highly skilled staff, time-consuming sample pretreatment, and sophisticated equipment, including atomic absorption spectrometry, inductively coupled plasma mass spectrometry (ICP-MS), surface-enhanced Raman scattering spectroscopy, and fluorescence.[13] These determination methods with the advantages of low detection limits and wide detection ranges are not suitable for on-site detection. Currently, simple and rapid on-site analytical approaches for soluble chromium are in high demand, which is mainly based on the colorimetric detection of Cr(VI). The most classic and favorite Cr(VI) chromogenic agent in visual detection is 1,5-diphenylcarbazide (DPC), which can produce a strong color change for quantitative or semiquantitative analysis.[14,15] DPC-based colorimetric detection has the advantages of high speed, simplicity, and low cost. However, its poor stability is also obvious, including strict storage conditions and short effective timeliness. Meanwhile, the signal strength

from the image acquisition equipment in colorimetric analysis could be seriously affected by the environment as the main source of a high signal-to-noise ratio.[7] Therefore, the visual chromogenic test paper should be combined with sophisticated preconcentration technology because its detection limit is not enough for assessing drinking water quality.[16,17] In this case, these shortages of DPC-based colorimetric detection from four main sources should be overcome for on-site visual detection of Cr(VI), including (a) short effective use time, poor sensitivity, and narrow linear range from unstable DPC, (b) unreliable reproducibility from chromogenic test paper, (c) environmental interference from image acquisition equipment, and (d) data insufficiency from DCNN.[18,19]

Therefore, we aim to solve the challenges of data-hungry DCNN and data quality via the optimization and synergism of a colorimetric Cr(VI) chemosensor (chemical analytical aspects) and the construction of FSL-based models (data processing aspects), and the latter is important for long-time-prepared, precious, small amount, chemical analysis data. This process is provided in the *supporting information*. A series of new strategies are proposed by us to overcome these obstacles, including (a) the protection of DPC by the blending of polyacrylonitrile (PAN) and thin-layer silica gel (SG) as a Cr(VI) color sensor (DPC/PAN/SG), (b) the electrospinning technology to prepare test paper with reliable reproducibility, (c) the obtaining of real sample pictures through dark boxes, structural light sources and high-stability and high-performance industrial cameras to minimize the sample noise caused by environmental changes, and (d) a new deep learning model for analytical chemistry, i.e., the combined technology of DCNN and GAN as FSL to improve the analytical performance with limited and real experimental data.

Materials and Methods

Chemical and Reagents. *N*-Dimethylformamide (DMF, 99 %), 1,5-diphenylcarbazide ($C_{13}H_{14}N_4O$, DPC), potassium dichromate ($K_2Cr_2O_7$), and the thin-layer chromatographic silica gel

(SG) were purchased from Xilong Chemistry Technology Co. Ltd. Polyacrylonitrile (PAN, M_w:150,000) was purchased from Sigma-Aldrich. All of them were analytically pure and directly used in the experiment. Ultrapure water was used during all experiments.

Apparatus. An electrospinning machine (LN-01C, Lvna Technology Co., Ltd. , China), a scanning electron microscope (SEM, Supra 55 sapphire, CARL ZEISS, German), a transmission electron microscope (FEI Tecnai F20, FEI Company, America), a constant-temperature magnetic agitator (LTD HWCL Type 1, Great Wall Technology & Trade Co., China), a solid-state UV-vis spectrophotometer (USB2000+, Ocean Optics, America), and a workstation (DELL Precision 3640 Tower 006, Dell Inc.) were used in this paper.

Preparation of Visualization Test Paper by Electrospinning. According to the literature [4,21] and experimental results in Figure S1, the optimal concentrations of precursor solutions were designed as follows. PAN (0.90 g), SG (0.30 g), and DPC (0.10 g) were completely dissolved in DMF (10 mL) by magnetic stirring at 60.0°C for 5.0 h, and then a thick and uniformly dispersed mixture was obtained for electrospinning. Before spinning, the temperature and the humidity were adjusted to 25.0°C and less than 50.0 %, respectively. The solution was inhaled into a syringe (10.0 mL), and an aluminum foil was wrapped with photoetching paper as the receiving plate. The injection pump propulsion speed and the voltage between the positive and negative electrodes were adjusted to 2.0 mL/h and 16.0 kV, respectively. Under the action of electrostatic gravity, the solution formed a Taylor cone at the tip of the syringe and pulled out a jet to accumulate uniformly on the surface of the receiving plate. After spinning, the nanofiber film was dried in a vacuum oven at 60.0°C for 2.0 h, and then the obtained visual test paper (DPC/PAN/SG) was cut into a size of 1.0 cm×1.0 cm as a Cr(VI) colorimetric sensor.

Construction of a Cr(VI) Determination System with a Colorimetric Sensor and a DL Tool.

Two hundred and thirty samples with uniform concentration distribution were prepared, with concentration gradients of 0.1000 and 0.0500 mg/L in the ranges of 0.0500-20.00 and 0.0500-0.1000 mg/L, respectivey. In addition, 861 real samples were also prepared in advance, whose concentration distribution was in the range of 0-20.00 mg/L. The samples (10 μL) were dropped on the visual test strip, and the standard plane-light was used to capture the sample images in the camera bellows. According to the influence of pH and hold time on the colorimetric reaction between DPC/PAN/SG and Cr(VI) (shown in Figure S2 and S3), the optimal pH value was 2, and the colorimetric reaction was complete after 30 s. To obtain high-quality sample data for improving the training accuracy and then the generation effect of the confrontation model, a camera bellows was assembled with a plane-structured light source and a high-stability industrial camera with 5 million pixels, and then the sample noise, e.g., uneven color spots and background interference, could be greatly reduced.

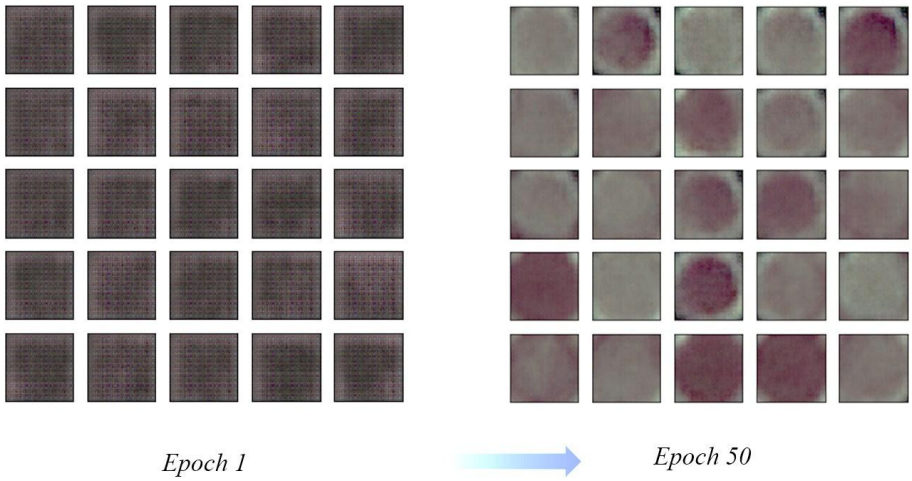

Figure 1. Improve Sample quality with the model-training process (epoch 1-50)

The sample image was labeled according to its concentration, and 230 and 861 pictures of standard and real samples were obtained, respectively, for training to generate the confrontation model, and then the standard sample database was prepared. The training set was a triplet of adjacent concentrations, and the elements of each triple could make any sample of the same

concentration (as shown in Figure 1). As a result, 13,500 “antagonistic samples” were generated. With the increase in model-training time, the quality of the sample image generated by the confrontation was also greatly improved to get close to the real sample, and the features gradually became obvious.

Both 13,500 of antagonistic sample images from GAN and 414 real sample images were randomly used as the training set, and the other 447 real sample images were used as the test set. By referring to the open-source model, DCNN as a high-performance and super-resolution tool was designed to “analyze” and “learn” the sample image signals, which was composed of an input layer, convolution layers, pooling layers, a full connection layer, and an output layer. The trained model could extract the color features of the colorimetric test paper from the image and classify it into a certain concentration. With the number of training increasing from 0 to 150 times, the loss value gradually decreased, and the training accuracy gradually increased to 85% (shown in Figure 2).

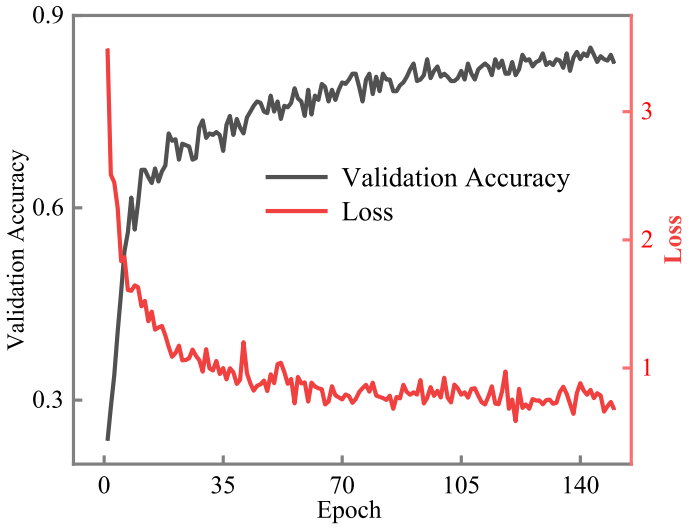

Figure 2. Training accuracy and loss value versus training number (epoch from 0 to 150)

The trained DCNN model was combined with smartphone software to realize the rapid analysis of the test data on-site. In the insitu test, the users could drop the sample onto the visual test paper,

capture images by a smartphone, and upload them on the APP, and then the prediction result of the DCNN model could be obtained within 10 s.

Results and Discussion

DPC-Based Colorimetric Detection Performance Comparison between Traditional Coating and DPC/PAN/SG. The stability and sensitivity of the colorimetric reaction depend to a great extent on the microstructure of nanomaterials, including the distribution and protection of the chromogenic agent, their specific surface area and hydrophilicity. By heating, stirring, and electrospinning, the chromogenic agent (DPC) can be effectively dissolved in DMF and uniformly mixed with a protective agent (PAN) and a hydrophilic carrier (SG). The stacking of nanofibers (DPC/PAN/SG) can be clearly seen by SEM images, and the diameters are uniformly distributed between 290 and 350 nm (Figure 3a), which brings a high specific surface area (53.43 m^2/g, Figure S4). When the water sample is dropped onto the test strip, due to the existence of a large number of hydroxyl groups on the surface of SG, its hydrophilicity is greatly improved (Figure S5), and the sample can infiltrate into the test paper quickly and evenly. Therefore, the reaction between DPC and Cr(VI) can be sufficient and fast. Comparing the TEM of DPC/PAN/SG before and after Cr(VI) detection (Figure S6), it can also be seen that DPC in the nanofibers could be dissolved into the water sample for the color reaction.

However, as one of the most commonly used chromogenic agents for Cr(VI) colorimetric detection, DPC is limited by its instability and active time, especially for on-site detection, because it should be isolated from the air and light. As a high-stability polymer, PAN is selected as the electrospinning substrate to blend, wrap, and stack the chromogenic agent of DPC, i.e., to block air into the visual test paper and then protect DPC before use, meanwhile, hydrophilic SG is also used as the carrier to guide Cr(VI) water samples into the visual test paper for the chromogenic reaction

between DPC. The stability of DPC in the visual test paper prepared with traditional coating on the SG plate and DPC/PAN/SG is tested by exposing under the same operating environment, including the same light, humidity, and air, and the results are shown in Figure S7. With the increase of the exposure time from 1 to 30 days, DPC loaded on the SG plate is deteriorates completely and fades, but the test strip of DPC/PAN/SG is still suitable for colorimetric detection. To verify the validity of DPC in the DPC/PAN/SG, the standard Cr(VI) solutions with different concentrations are dropped onto the test strip and scanned by solid-state ultraviolet. As shown in Figure 3b, the significant ultraviolet absorptions in the range of 540-560 nm with the maximum absorption band at 540 nm are observed, and the absorption intensities are proportional to Cr(VI) concentration, which is similar to DPC used alone.[14] It is proved that the complexation reaction between DPC and Cr(VI) is not affected by its blending with PAN and SG.

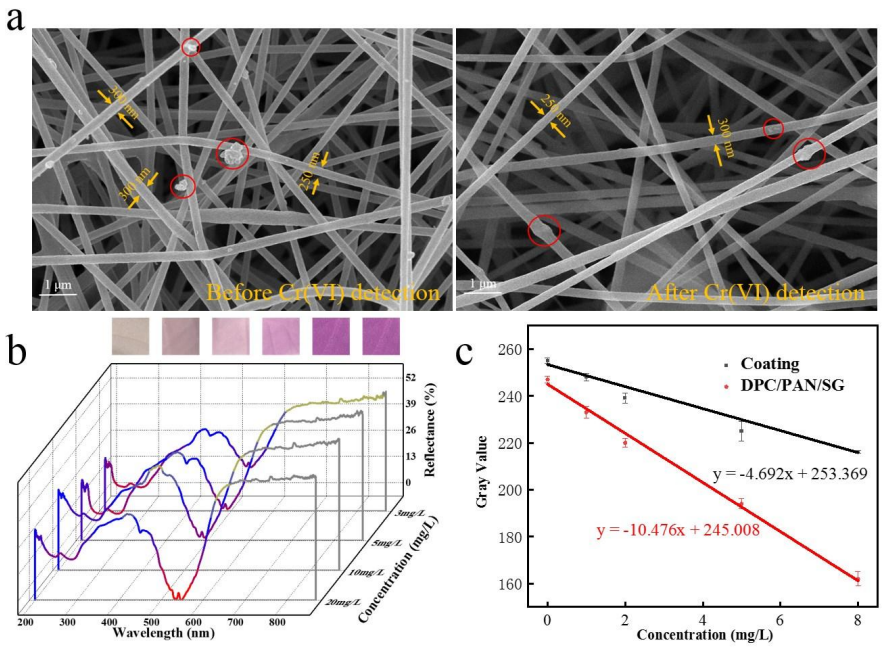

Figure 3. (a) SEM of DPC/PAN/SG before (left) and after (right) Cr(VI) detection. (b) Solid ultraviolet scanning spectrogram of DPC/PAN/SG with different Cr(VI) concentration. (c) Gray value-based standard curves of visual test strips prepared by different methods.

The colorimetric detection performances of two kinds of DPC-based test papers, including

traditional SG coating and DPC/PAN/SG, are compared with the Euclid Distance method. After adding Cr(VI) (0-8.000 mg/L) onto the test paper, the gray value of each color spot is recorded via Photoshop software, and then a linear correlation between the Cr(VI) concentrations and gray values is found, with a high correlation coefficient (R^2 >0.99, Figure 3c). According to the linear slope, the colorimetric detection sensitivity of DPC/PAN/SG is better than that of SG coating, and their detection limits are 1.571 and 3.738 mg/L, respectively, i.e., the colorimetric reaction active sites and rate between DPC and Cr(VI) could be improved by more than 2.0 times by the blending of PAN and SG and electrospinning for the increase in specific surface area. In addition, the anti-interference ability of DPC/PAN/SG for selective determination of Cr(VI) is excellent, under the optimum reaction conditions. The influence of coexisting ions (29 kinds [22-25]) on the color and gray value change (ΔG) on DPC /PAN /SG after the reaction with Cr(VI) (10 mg/L), i.e., colorimetric determination, is not obvious (shown in Figure 4).

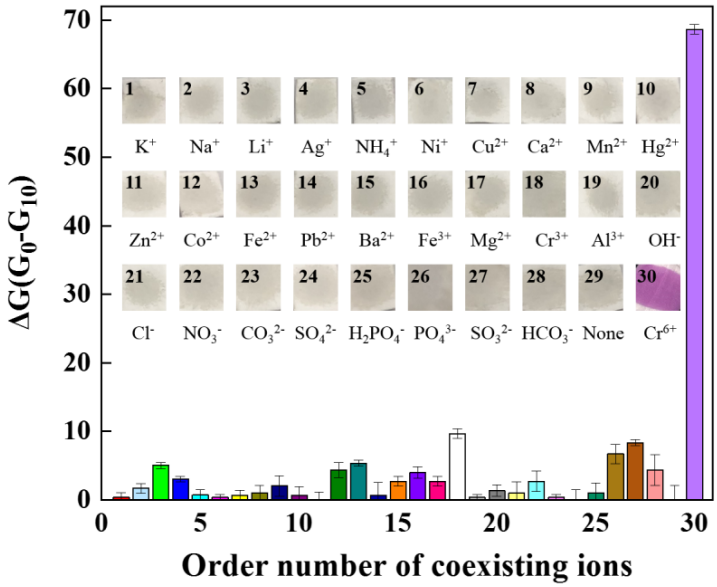

Figure 4. Color and gray value change (ΔG) on DPC/PAN/SG after the reaction with Cr(VI) (10 mg/L), adding the coexisting ions (1 mg/L for Fe^{2+} and Fe^{3+}, 10 mg/L for other ions; n = 3).

At present, the detection limits of DPC-based dipstick tests for Cr(VI) without additional

enrichment are reported in the range of 3.000-10.00 mg/L,[4] which is difficult to meet the requirement of WHO and USEPA. Therefore, gray value-based signal processing technology for the sample images should be replaced by the deep learning method.

Few-Shot Learning-Based Data Tool for Cr(VI) Colorimetric Detection. DCNN, as one-click image analysis with super-resolution, has already revolutionized colorimetric determination. [4,5] But it is severely limited by its data-hungry nature, which is overcome by combining the GAN with DCNN, i.e., FSL is proposed as a new data tool.

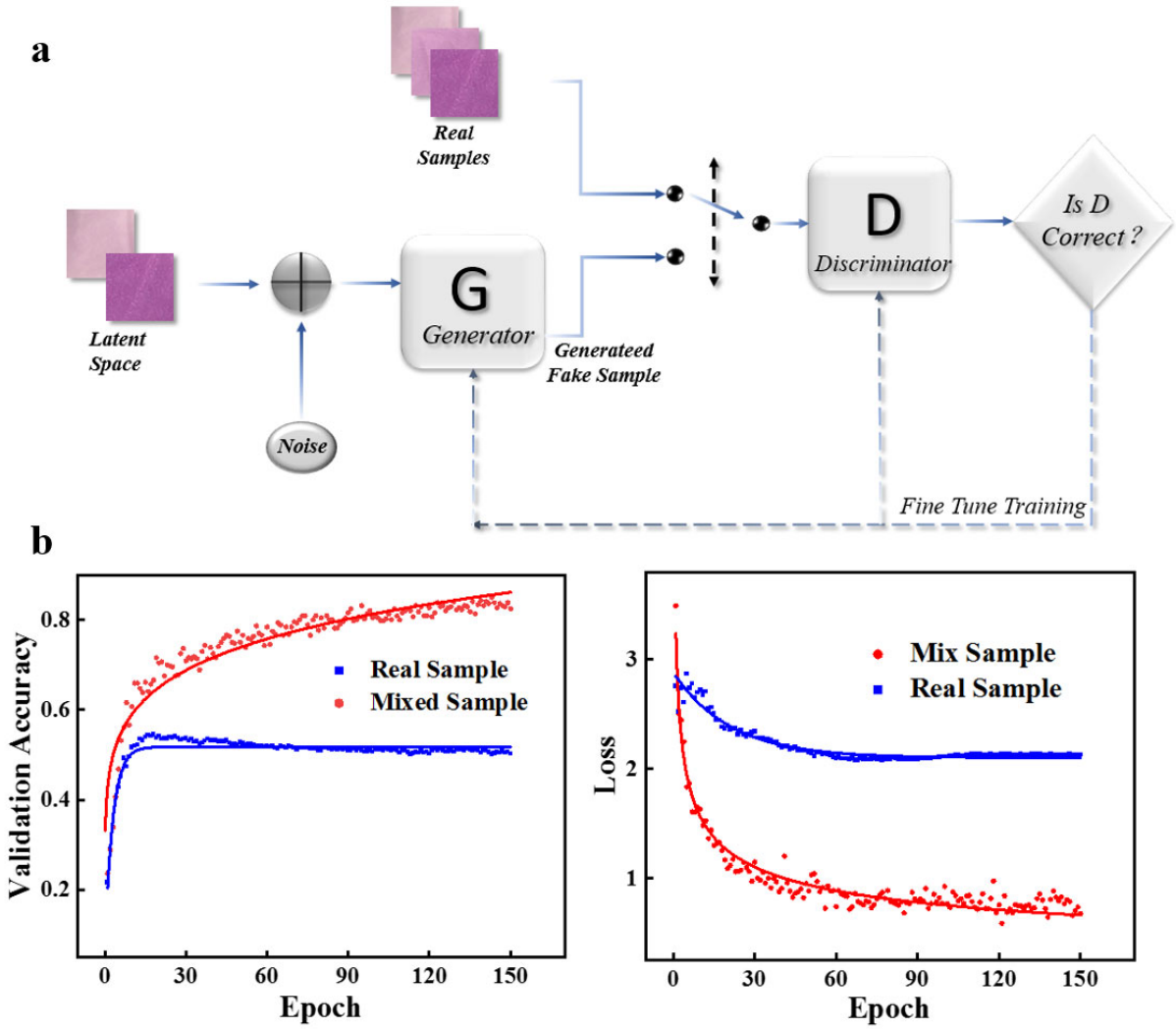

Figure 5. (a) Structure of GAN. (b) Validation accuracy (left) and loss (right) vs DCNN training

number (epoch from 0 to 150).

The developed GAN is mainly composed of two parts, including a generator and a discriminator. A series of data groups from real samples are used, including three different concentrations, i.e., a higher concentration, a lower concentration and an intermediate concentration between them. The generator only gets the data from the higher and lower concentrations and generates a “noise”, i.e., fake sample data, as the output, which is similar to the intermediate sample. They are designed to produce very realistic images, which are especially difficult to identify by the eye. This noise acts as the intermediate concentration and forms a complete data group for the judgment of its accuracy with the discriminator. The discriminator gets both the real and the generated data as input, which come from the training set from real and generated samples, respectively. In brief, the generator tries to generate realistic samples, and the discriminator makes a correct judgment during the training process (Figure 5a). After 100 cycles of training, the simulation effect is shown in Figure 5b, the accuracy is greatly improved. While selecting the sample generation method, the commonly used convolution self-encoder (CSE) method is also tested, using the same train samples. In the 100th training, CSE is able to extract and generalize the feature information via the comparison between the samples, but its generated image quality is poorer than that with GAN, according to the comparison among real samples and their corresponding generated samples with GAN and CSE in Figure 6. Therefore, the GAN model is chosen for the generation of sample images with full concentrations from 0 to 20.00 mg/L.

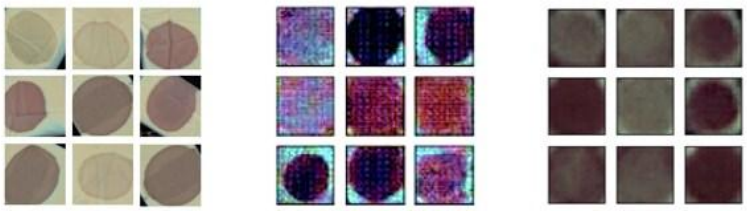

Real CSE Few-shot Learning

Figure 6. Comparison of real samples and their corresponding generated samples with CSE and FSL.

As an open-source database, a new DCNN model with five convolutions and five pooling is designed to improve its ability for extracting sample features and reducing its calculation quantity. The increase in the number of real samples is important to improve the learning effect of the DCNN model and judge the generated sample effect of the GAN, resulting in a sharp increase in workload. The use of antagonistic sample images solves this problem and also complements the samples with unknown concentrations. Therefore, an appropriate quantity and quality of samples, including both real and antagonistic samples, on the prediction effect are important. The same test set and different training sets are used to train two models of DCNN and train 150 times to compare their accuracies and loss function changes. The first model uses 414 real samples as the training set, and the second model uses the same 414 real samples plus 13,500 antagonistic samples as the training set. In addition, the same 447 nonrepetitive real samples as the test set are applied by these two models. The above samples as the test and training sets are randomly selected from all 861 real samples. The variation curves of the training accuracy and loss rate of these two training sets are obtained for the same DCNN model. With the addition of large generated samples (13,500 of antagonistic samples) into the training set (only 414 real samples), the training accuracy could be increased from 51.26 to 85.00%, after epoch 150 in the detection range of 0.050-20.00 mg/L, as shown in Figure 5b. The accuracy of 85.00% is enough for the microdetection with colorimetry. Therefore, the limit of data-hungry from DCNN could be overcome by combining with GAN, i.e., FSL.

Analytical Performance of the Colorimetric Cr(VI) Chemosensor. To verify the practicability and accuracy of our intelligent analysis platform, drinking water and river water are tested as real samples. 500 mL of samples are pretreated for the determination of Cr(VI), according

to the preprocessing process shown in the *supporting information*. The results and their comparisons with ICP-MS are shown in Table 1. The result of our intelligent analysis platform is consistent with that of ICP-MS, and the recovery is between 99.60 and 101.8%. The influence of the coexisted organic matter and metals in drinking and river water on the analytical performance is not observed and it might be due to the advantage of DPC-based colorimetric detection. Here, the detectability and high performance of hyphenated techniques based on the DPC-based chemosensor and FSL for Cr(VI) detection have a great improvement in analytical performance.

After the protection of DPC with the blending of PAN and SG and its reliable reproducibility via electrospinning, the colorimetric detection performance of the DPC-based Cr(VI) color sensor is improved. Compared with using DPC/PAN/SG alone, the detection limit of its combination with FSL is further optimized from 1.571 to 0.050 mg/L. Using traditional measurement methods (including ED methods or the naked eye) to discriminate color data is far inferior to using machine learning for analysis, because they could be disturbed by environmental noise, and then their color features will be subjected to certain fluctuations. The color blocks in different positions of the same sample image, especially in the edge and center, will be different due to the slow infiltration of the sample and the difference in light scattering for unavoidable material heterogeneity. If these environmental noises cannot be effectively avoided and the color feature information can be accurately extracted, the outcome of color block-based data analysis by traditional measurement methods will be greatly reduced and varied. FSL tools benefit from their whole sample image-based characterization and powerful feature extraction capabilities, and then the detection accuracy and detection limit of DPC-based chemical sensors could be greatly optimized. Even without enrichment processing for avoiding its time consumption and easy contamination, the detection limit of Cr(VI) in the drinking water can meet on-site detection requirements by USEPA, WHO and

China. Furthermore, FSL, as a new DL tool for solving the data-hungriness of DCNN, will be emerged as the indisputable leader for colorimetric analysis.

Table 1. Determination of Cr(VI) in 500 mL of Natural Water Samples

water samples	added (mg)	found (mg)	RSD (%，*n*=9)	recovery (%)	found by ICP-MS (mg)	RSD (%, *n*=9)
drinking water	0	0	0	-	0.009	2.594
	2.500	2.556	5.842	99.6	2.531	1.535
	5.000	4.815	6.044	101.8	5.010	0.613
river water	0	0.005	5.694	-	0.023	3.475
	2.500	2.454	1.887	97.1	2.563	2.330
	5.000	5.076	2.238	100.5	5.014	3.505

Conclusions

Through the combination of GAN and DCNN, a new DL method as FSL is proposed for the first time, and then an accuracy, intelligent and chemosensor-based analysis platform is quickly built, just based on a small number of sample images. Compared with DCNN with the same real samples and training level, our FSL model has higher accuracy, faster learning efficiency and lower training loss. Compared with the traditional ED method with DCNN, our analytical performance, including the detection limit and the detection range, could be significantly improved, for FSL with whole sample image-based characterization and powerful feature extraction capabilities. It has been successfully applied for the visual detection of Cr(VI) in natural water, after smartphone APP-based data collection. If FSL is used with blockchain technology for secure data end-to-end connectivity and management, [20] on-site water environment monitoring systems for Cr(VI) could be established.

With the combination of PAN, DPC, and SG via electrospinning technology, a new DPC-based chemosensor is obtained, with the advantages of high stability, enough hydrophilicity, fast reaction speed, good repeatabillity and so on. The time for the full determination process, i.e., from addition of the sample to obtain the final result, can be shortened to 3 min. Such improvements of popular

DPC-based chemosensors enhance the quality of the sample images and lengthen the effective time for more than 30 days, making them convenient, fast, low-cost. Thus, this chemosensor is suitable for intelligent and visual on-site detection.

Acknowledgements

This work was supported by the National Natural Science Foundation of China (22074058, S.X.L) and the Project of Industry-University-Research Cooperation of Fujian Province (2019Y4010, F.J.L).

Author contributions

‖ Z.-J.H. and § Hao Li H.L. contributed to the work equally and should be regarded as co-first authors. S.-X.L. conceived the project. Z.-J.H. designed the photocatalysis and colorimetry sensor. H.L. designed the few-shot learning model for colorimetric determination. F.L. supervised the research. All authors proofread the manuscript and provided comments.

Competing interests

The authors declare no competing financial interest.

Additional information

Supplementary information. The Supporting Information of the DCNN and GAN model is available free of charge. In addition, the preprocessing of actual samples and the comparison of real sampleS and their corresponding generated samples with GAN and CSE are also included.

Correspondence and requests for materials should be addressed to Shunxing Li.

REFERENCE

(1) Schmidt, J.; Marques, M. R.; Botti, S.; Marques, M. A. Recent advances and applications of machine learning in solid-state materials science. *npj Comput. Mater.* **2019**, 5(1), 1-36.

(2) Jumper, J.; Evans, R.; Pritzel, A.; et al.. Highly accurate protein structure prediction with AlphaFold. *Nature* **2021**, 596(7873), 583-589.

(3) Debus, B.; Parastar, H.; Harrington, P.; ... & Kirsanov, D. Deep learning in analytical chemistry. *TrAC, Trends Anal. Chem.* **2021**, 145, 116459.

(4) Luo J. Y.; Huang Z. J.; Li S. X.; Zheng F. Y.; Liu F. J.; Huang Q. Y.; Huang X. G.; Xie H. J. Photodegradation Kinetics and Deep Learning-Based Intelligent Colorimetric Method for Bioavailability-Based Dissolved Iron Speciation. *Anal. Chem.* **2022**, 94(42), 14801-14809.

(5) Huang Z. J.; Luo J. Y.; Zheng F. Y.; Li S. X.; Liu F. J.; Lin L. X.; Huang Y. J.; Man S.; Cao G. X.; Huang X.G. Long-term stable, high accuracy, and visual detection platform for In-field analysis of nitrite in food based on colorimetric test paper and deep convolutional neural networks. *Food Chem.* **2022**, 373, 131593.

(6) Aryandoust, A.; Patt, A.; ... & Pfenninger, S. Enhanced spatio-temporal electric load forecasts using less data with active deep learning. *Nat. Mach. Intell.* **2022**, 4, 977–991.

(7) Laine, R. F.; Arganda-Carreras, I.; Henriques, R.; ... & Jacquemet, G. Avoiding a replication crisis in deep-learning-based bioimage analysis. *Nat. Methods* **2021**, 18(10), 1136-1144.

(8) Yi X; Walia E; Babyn P. Generative adversarial network in medical imaging: A review. *Med. Image Anal.* **2019**, 58, 101552.

(9) Yang, W.; Zhang, X.; Tian, Y.; Wang W.; Xue, J. H.; ... & Liao, Q. Deep learning for single image super-resolution: A brief review. *IEEE Trans. Multimedia* **2019**, 21(12), 3106-3121.

(10) Springthorpe, S. K.; Dundas, C. M.; ... & Keitz, B. K. Microbial reduction of metal-organic

frameworks enables synergistic chromium removal. *Nat. Commun.* **2019**, 10(1), 1-11.

(11) Yao, L.; Hu, Y.; Zou, Y.; Ji, Z.; Hu, S.; Wang, C.; ... & Wang, X. Selective and efficient photoextraction of aqueous Cr (VI) as a solid-state polyhydroxy Cr (V) complex for environmental remediation and resource recovery. *Environ. Sci. Technol.* **2022**, 56(19), 14030-14037.

(12) Zheng, F. Y.; Lin, X. F.; Yu, H. W.; Li, S. X.; Huang, X. G. Visible-light Photoreduction, Adsorption, Matrix Conversion and Membrane Separation for Ultrasensitive Chromium Determination in Natural Water by X-ray Fluorescence. *Sens. Actuators, B* **2016**, 226, 500-505.

(13) Zhuang, Y. T.; Chen, S.; Jiang, R.; Yu, Y. L.; Wang, J. H. Ultrasensitive colorimetric chromium chemosensor based on dye color switching under the Cr(VI)-Stimulated Au NPs catalytic activity. *Anal. Chem.* **2019**, 91, 5346−5353.

(14) Kim, B. M.; Kim, B.; Nam, S. E.; Eom, H. J.; Lee, S.; Kim, K.; ... & Rhee, J. S. Reductive Transformation of Hexavalent Chromium in Ice Decreases Chromium Toxicity in Aquatic Animals. *Environ. Sci. Technol.* **2022**, *56*(6), 3503-3513.

(15) Alahmad, W.; Sahragard, A.; & Varanusupakul, P. An overview of the recent developments of microfluidic paper-based analytical devices for the detection of chromium species. *Microchem. J.* **2021**, 170, 106699.

(16) Tan W.; Xu Z.; Zhang L.; Shen W. Trace analysis on chromium (VI) in water by pre-concentration using a superhydrophobic surface and rapid sensing using a chemical-responsive adhesive tape. *Talanta* **2020**, 218, 121116.

(17) Alahmad W.; Varanusupakul P.; Kaneta T.; Varanusupakul P. Chromium speciation using paper-based analytical devices by direct determination and with electromembrane microextraction. *Anal. Chim. Acta* **2019**, 1085, 98-106.

(18) Zhang, Y.; Zhu, Y.; Zeng, Z.; Zeng, G.; Xiao, R.; Wang, Y.; ... & Feng, C. Sensors for the

environmental pollutant detection: Are we already there?. *Coord. Chem. Rev.* **2021**, 431, 213681.

(19) Chen, S.; Jiang, T.; Lin, H.; Chen, J.; Yang, S.; Wang, P.; ... & Fang, Y. Fast and Ultrasensitive Visual Detection of Exosomes in Body Fluids for Point-of-Care Disease Diagnosis. *Anal. Chem.* **2021**, 93(29), 10372-10377.

(20) Guo, X.; Khalid, M. A.; Domingos, I.; Michala, A. L.; Adriko, M.; Rowel, C.; ... & Cooper, J. M. Smartphone-based DNA diagnostics for malaria detection using deep learning for local decision support and blockchain technology for security. *Nat. Electron.* **2021**, 4(8), 615-624.

(21) Shi, S.; Si, Y.; Han, Y.; Wu, T.; Iqbal, M. I.; Fei, B.; ... & Qu, J. Recent progress in protective membranes fabricated via electrospinning: advanced materials, biomimetic structures, and functional applications. *Adv. Mater.* **2022**, 34(17): 2107938.

(22) Zhang, T. ; Zhang, S. ; Liu, J. ; Li, J. ; & Lu, X. Efficient visual chemosensor for hexavalent chromium via a controlled strategy for signal amplification in water. *Anal. Chem.* **2020**, 92(4), 3426-3433.

(23) Liu, M. ; Zhang, S. ; Wang, Y. ; Liu, J. ; Hu, W. ; & Lu, X. Hexavalent chromium as a smart switch for peroxidase-like activity regulation via the surface electronic redistribution of silver nanoparticles anchored on carbon spheres. *Anal. Chem.* **2022**, 94(3), 1669-1677.

(24) Scindia, Y. M. ; Pandey, A. K. ; Reddy, A. V. R. ; & Manohar, S. B. Selective preconcentration and determination of chromium (VI) using a flat sheet polymer inclusion sorbent: potential application for Cr (VI) determination in real samples. *Anal. Chem.* **2002**, 74(16), 4204-4212.

(25) Wang, Y. ; Liang, R. P. ; & Qiu, J. D. Nanoceria-templated metal organic frameworks with oxidase-mimicking activity boosted by hexavalent chromium. *Anal. Chem.* **2020**, 92(2), 2339-2346.